National Conference with International Participation
ENGINEERING MECHANICS 2007
Svratka, Czech Republic, May 14 – 17, 2007

FORCED VIBRATION OF BLADED DISK

J. Kellner, J.Šašek, V. Zeman*

Summary: *The paper presents the modal synthesis method for a mathematical modelling of rotating bladed disk vibration. The standard finite element software does not allow to consider all effects of the rotation. The presented method makes it possible to respect Coriolis and centrifugal forces acting continuously on the three-dimensional elastic disk and one-dimensional elastic blades connected together at the top with shrouds. A centrifugal blade stiffening is considered. The method is applied to the steady forced vibration of the real rotating bladed disk excited by aerodynamic forces.*

1. Introduction

Many rotating systems are modelled as one-dimensional rotating bodies with rigid disks attached to them as is shown for example in publications of Krämer (1993) and Yamamoto & Ishida (2001). However, there are cases in which the high-frequency modes of rotating bodies cannot be neglected. Typical example is the bladed disk in turbomachines excited by aerodynamic and hydrodynamic forces (Birget, 2001). One of the newest and more comprehensive publications is monograph of Genta (2005), where the three-dimensional modelling of rotors is described in more details. In this monograph the author prefers a discretization of an axially symmetrical rotors using annular axi-symmetric elements. This approach cannot be applied for discretization of the bladed disks.

The aim of this article is to develop suitable methodology for forced vibration modelling of the rotating bladed disk using experience with discretization of 3D rotating disks Šašek et al., (2006), modelling the rotating blade Kellner & Zeman (2006), modal analysis of the bladed disk (Zeman et al., 2007) and with applications of the modal synthesis method in dynamics of machines (Zeman, 2005). The recent advances in CFD/FEM software and hardware allowed the computation of the fluid-flow introduced forces and resulting stresses in turbomachinery blades (see Misek et al., 2007). The calculated time-dependent pressure distribution is then used for forced response of the bladed disk.

2. Mathematical model of the rotating bladed disk

The rotating bladed disk can be generally decomposed into disk (subsystem D) and separated blade packets (subsystems $P_s,\ s = 1, 2, \dots, p$), where p is their count (Fig. 1). We assume that the disk is centrally clamped into turbomachine rotor rotating with constant angular speed ω. The disk nodes on the inner radius are fixed in all directions. The blades (B_j) in packets (P_s) are connected on the top with shrouds (S). The blades elastic seating to disk is replaced

* Ing. Josef Kellner, Ing. Jakub Šašek, Prof. Ing. Vladimír Zeman, DrSc., Department of Mechanics, Faculty of Applied Sciences, University of West Bohemia in Pilsen, Univerzitní 8, 306 14 Plzeň, tel. +420 377 63 23 15, fax: +420 377 632 302, e-mail: kennyk@kme.zcu.cz

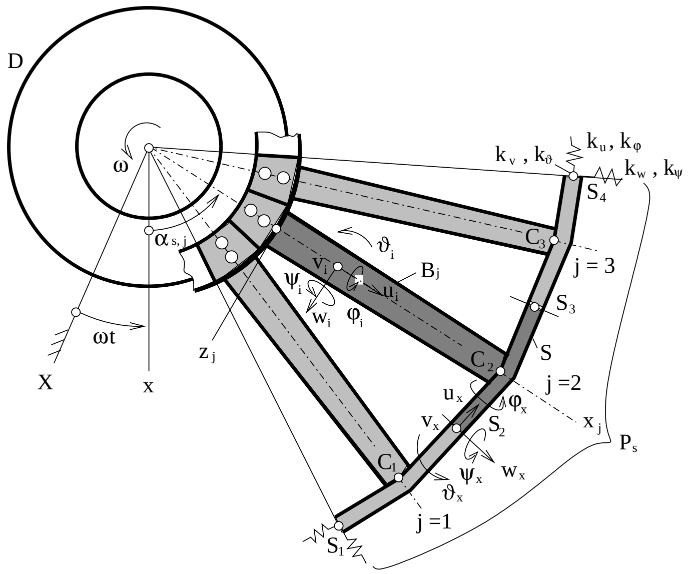

Figure 1: Scheme of the bladed disk with detail of one blade packet.

with elastic supports in outer contact points of two dog bolts between disk and every one blade foot. The blade packets are mutually connected by elastic linkages characterized by diagonal stiffness matrix $\boldsymbol{K}_L = diag(k_u,\, k_v,\, k_w,\, k_\varphi,\, k_\vartheta,\, k_\psi)$.

The mathematical model of the undamped subsystems incorporated in the rotating bladed disk can be written in matrix form Šašek et al., (2006), Zeman & Kellner (2006)

$$\boldsymbol{M}_D\ddot{\boldsymbol{q}}_D(t) + \omega\boldsymbol{G}_D\dot{\boldsymbol{q}}_D(t) + \left(\boldsymbol{K}_{\mathbf{s}D} - \omega^2\boldsymbol{K}_{dD}\right)\boldsymbol{q}_D(t) = \omega^2\boldsymbol{f}_D + \boldsymbol{f}_D^C \tag{1}$$

$$\boldsymbol{M}_P\ddot{\boldsymbol{q}}_{P,s}(t)+\omega\boldsymbol{G}_P\dot{\boldsymbol{q}}_{P,s}(t)+\left(\boldsymbol{K}_{\mathbf{s}P} - \omega^2\boldsymbol{K}_{dP} + \omega^2\boldsymbol{K}_{\omega P}\right)\boldsymbol{q}_{P,s}(t) = \omega^2\boldsymbol{f}_P+\boldsymbol{f}_{P,s}^C+\boldsymbol{f}_{P,s}(t), \tag{2}$$

$$s{=}1,2,\ldots,p,$$

where mass matrices $\boldsymbol{M}_D,\, \boldsymbol{M}_P$, static stiffness matrices $\boldsymbol{K}_{\mathbf{s}D}, \boldsymbol{K}_{\mathbf{s}P}$ and dynamic stiffness matrices $\boldsymbol{K}_{dD},\, \boldsymbol{K}_{dP}$ of the disk (subscript D) and blade packets (subscript P) are symmetrical. Symmetric matrix $\boldsymbol{K}_{\omega P}$ expresses a centrifugal blade stiffening (see in Kellner & Zeman (2006)). Skew-symmetric matrices $\omega\boldsymbol{G}_D$ and $\omega\boldsymbol{G}_P$ express gyroscopic effects. Centrifugal load vectors $\omega^2\boldsymbol{f}_D$ and $\omega^2\boldsymbol{f}_P$ are constant in time. Vectors $\boldsymbol{f}_{P,s}(t)$ express the excitation of the blade packets by aerodynamic forces. All presented matrices in models (1) and (2) correspond to mutually uncoupled subsystems and are created by means of finite element method (for more details see contributions Šašel et al., (2006), Kellner & Zeman (2006) and Zeman & Kellner (2006)). Vectors $\boldsymbol{f}_D^C$ and $\boldsymbol{f}_{P,s}^C$ ($s = 1, 2, \ldots, p$) represents the coupling forces in general coordinates of subsystems

$$\boldsymbol{q}_D = \left[\ldots\; u_i^{(D)}\; v_i^{(D)}\; w_i^{(D)}\; \ldots\right]^T \in \mathcal{R}^{n_D} \tag{3}$$

$$\boldsymbol{q}_{P,s} = \left[\boldsymbol{q}_{S_1}^T\boldsymbol{q}_{B,1}^T\boldsymbol{q}_{S_2}^T\boldsymbol{q}_{B,2}^T\boldsymbol{q}_{S_3}^T\boldsymbol{q}_{B,3}^T\boldsymbol{q}_{S_4}^T\right]_{P,s}^T \in \mathcal{R}^{n_P} \tag{4}$$

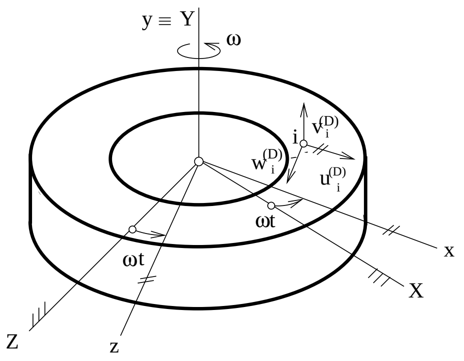

Figure 2: Scheme of the disk.

where $u_i^{(D)}$, $v_i^{(D)}$, $w_i^{(D)}$ in (3) are disk nodal displacements in direction of disk rotating axis x, y, z (Fig. 2). Coordinates of subvectors $\boldsymbol{q}_{B,j}$ ($j = 1,2,3$) express the blade displacements of the node i (Fig. 1) in direction of rotating axis x_j, y_j, z_j and small turn angles of the blade cross section (subscript j corresponds to blade in packet)

$$\boldsymbol{q}_{B,j} = [\dots\ u_i\, v_i\, w_i\, \varphi_i\, \vartheta_i\, \psi_i\ \dots]_{B,j}^T\ , \quad i = 1,2,\dots,N, \quad j = 1,2,3. \tag{5}$$

Coordinates of subvectors $\boldsymbol{q}_{S_1}$,$\boldsymbol{q}_{S_{2,\dots}}$ express the shroud's displacements in nodes $S_1,\ S_2,\dots$

$$\boldsymbol{q}_x = [u_x\ v_x\ w_x\ \varphi_x\ \vartheta_x\ \psi_x]_{P,s}^T\ , \quad x = S_1,\ S_2,\dots \tag{6}$$

Vector $\boldsymbol{f}_D^C$ represents the forces in all blade's seating to disk acting on the disk. Vector $\boldsymbol{f}_{P,s}^C$ expresses the coupling forces in blade's seating of packet P,s and in shroud linkages between blade packets acting on single packet P,s. The global coupling force vector in global configuration space of all general coordinates

$$\boldsymbol{q} = \left[\boldsymbol{q}_D^T\ \boldsymbol{q}_{P,1}\ \boldsymbol{q}_{P,2}\ \dots \boldsymbol{q}_{P,p}\right]^T \tag{7}$$

can be calculated from the potential (strain) energy as

$$\boldsymbol{f}_C = \begin{bmatrix} \boldsymbol{f}_D^C \\ \boldsymbol{f}_{P,1}^C \\ \vdots \\ \boldsymbol{f}_{P,p}^C \end{bmatrix} = -\frac{\partial E_p^C}{\partial \boldsymbol{q}}\ . \tag{8}$$

This energy can be expressed in the additive form

$$E_p^C = \sum_{s=1}^{p} \sum_{j=1}^{b} E_{s,j}^C + E_P^C\,, \tag{9}$$

where $E_{s,j}^C$ is coupling strain energy between blade j in blade packet s and the disk and the E_P^C is strain energy of all shroud linkages between blade packets. The linearized global coupling force vector can be written in the form

$$\boldsymbol{f}_C = -\sum_{s=1}^{p} \sum_{j=1}^{b} \boldsymbol{K}_{s,j}^C \boldsymbol{q} - \boldsymbol{K}_P^C \boldsymbol{q}\,. \tag{10}$$

The coupling stiffness matrices result from equations

$$\frac{\partial E_{s,j}^C}{\partial \boldsymbol{q}} = \boldsymbol{K}_{s,j}^C \boldsymbol{q}\,, \quad \frac{\partial E_P^C}{\partial \boldsymbol{q}} = \boldsymbol{K}_P^C \boldsymbol{q}\,. \tag{11}$$

The mathematical models (1), (2) using (8) and (10) after completion of a damping can be rewritten in the global matrix form

$$\begin{bmatrix} \boldsymbol{M}_D & \mathbf{0} \\ \mathbf{0} & \boldsymbol{M}_R \end{bmatrix} \begin{bmatrix} \ddot{\boldsymbol{q}}_D(t) \\ \ddot{\boldsymbol{q}}_R(t) \end{bmatrix} + \left(\begin{bmatrix} \boldsymbol{B}_D & \mathbf{0} \\ \mathbf{0} & \boldsymbol{B}_R \end{bmatrix} + \omega \begin{bmatrix} \boldsymbol{G}_D & \mathbf{0} \\ \mathbf{0} & \boldsymbol{G}_R \end{bmatrix} \right) \begin{bmatrix} \dot{\boldsymbol{q}}_D(t) \\ \dot{\boldsymbol{q}}_R(t) \end{bmatrix} +$$

$$+ \left(\begin{bmatrix} \boldsymbol{K}_D(\omega) & \mathbf{0} \\ \mathbf{0} & \boldsymbol{K}_R(\omega) \end{bmatrix} + \sum_{s=1}^{p} \sum_{j=1}^{b} \boldsymbol{K}_{s,j}^C \right) \begin{bmatrix} \boldsymbol{q}_D(t) \\ \boldsymbol{q}_R(t) \end{bmatrix} = \omega^2 \begin{bmatrix} \boldsymbol{f}_D \\ \boldsymbol{f}_C \end{bmatrix} + \begin{bmatrix} \mathbf{0} \\ \boldsymbol{f}_R(t) \end{bmatrix} \quad (12)$$

where

$$\boldsymbol{q}_R = \left[\boldsymbol{q}_{P,1}^T \quad \boldsymbol{q}_{P,2}^T \ \dots \ \boldsymbol{q}_{P,p}^T \right]^T \in \mathcal{R}^{n_R}, \ n_R = p\, n_P \quad (13)$$

is the general coordinate vector of a blading with shroud creating the blade rim (subscript R). The global stiffness matrix of the rotating disk has the form

$$\boldsymbol{K}_D(\omega) = \boldsymbol{K}_{\mathbf{s}D} - \omega^2 \boldsymbol{K}_{dD} \in \mathcal{R}^{n_D, n_D} . \quad (14)$$

The matrices of the blade rim are compiled from the blade packet matrices

$$\boldsymbol{X}_R = diag\,(\boldsymbol{X}_P,\ \boldsymbol{X}_P, \dots \boldsymbol{X}_P,\ ) \in \mathcal{R}^{n_R, n_R},\ \boldsymbol{X} = \boldsymbol{M}, \boldsymbol{G}, \boldsymbol{K}_{\mathbf{s}}, \boldsymbol{K}_d, \boldsymbol{K}_\omega . \quad (15)$$

The global stiffness blade rim matrix is

$$\boldsymbol{K}_R(\omega) = \boldsymbol{K}_{\mathbf{s}R} + \omega^2 \left(\boldsymbol{K}_{\omega R} - \boldsymbol{K}_{dR} \right) + \boldsymbol{K}_{PP}^C \in \mathcal{R}^{n_R, n_R}, \quad (16)$$

where $\boldsymbol{K}_{PP}^C$ is the coupling stiffness matrix of all shroud linkages between blade packets satisfying the equation

$$\frac{\partial E_p^C}{\partial \boldsymbol{q}_R} = \boldsymbol{K}_{PP}^C \boldsymbol{q}_R . \quad (17)$$

The centrifugal load vector of the blade rim is

$$\boldsymbol{f}_C = \left[\boldsymbol{f}_P^T \ \boldsymbol{f}_P^T \ \dots \ \boldsymbol{f}_P^T \right]^T \in \mathcal{R}^{n_R} \quad (18)$$

and vector of the aerodynamic forces has the general form

$$\boldsymbol{f}_R(t) = \left[\boldsymbol{f}_{P,1}^T(t),\ \boldsymbol{f}_{P,2}^T(t),\ \dots,\ \boldsymbol{f}_{P,p}(t) \right]^T \in \mathcal{R}^{n_R} . \quad (19)$$

It is advantageous to assemble condensed mathematical model of the rotating bladed disk with reduced degrees of freedom (DOF) number, because mainly the three-dimensional elastic disk could have large DOF number n_D and blade rim DOF number is $n_R = p\, n_P$.

The modal transformations

$$\boldsymbol{q}_D(t) = {}^m\boldsymbol{V}_D \boldsymbol{x}_D(t), \quad \boldsymbol{q}_R(t) = {}^m\boldsymbol{V}_R \boldsymbol{x}_R(t) \quad (20)$$

are introduced for this purpose. Matrices ${}^m\boldsymbol{V}_D \in \mathcal{R}^{n_D, m_D}$ and ${}^m\boldsymbol{V}_R \in \mathcal{R}^{n_R, m_R}$ are "master" modal submatrices of subsystems D (disk) and R (blade ring) obtained from modal analysis of the mutually uncoupled ($\boldsymbol{K}_{s,j}^C = \mathbf{0}$ for all $s,\ j$) and non-rotating subsystems represented by models

$$\boldsymbol{M}_D \ddot{\boldsymbol{q}}_D(t) + \boldsymbol{K}_{\mathbf{s}D} \boldsymbol{q}_D(t) = \mathbf{0}, \quad \boldsymbol{M}_R \ddot{\boldsymbol{q}}_R(t) + \left(\boldsymbol{K}_{\mathbf{s}R} + \boldsymbol{K}_{PP}^C \right) \boldsymbol{q}_R(t) = \mathbf{0} . \quad (21)$$

A condensation (reduction in DOF number) of both systems is attached by selection of a set of m_D and m_R subsystem master mode shapes ($m_D < n_D$, $m_R < n_R$). The new configuration space of dimension $m = m_D + m_R$ is defined by vector

$$\boldsymbol{x}(t) = \left[\boldsymbol{x}_D^T(t) \quad \boldsymbol{x}_R^T(t)\right]^T \in \mathcal{R}^m . \tag{22}$$

After the transformations (20) with considerations of the orthonormality conditions ${}^m\boldsymbol{V}_D^T \boldsymbol{M}_D \, {}^m\boldsymbol{V}_D = \boldsymbol{E}_D$ and ${}^m\boldsymbol{V}_R^T \boldsymbol{M}_R \, {}^m\boldsymbol{V}_R = \boldsymbol{E}_R$ the model (12) can be rewritten in the condensed form

$$\begin{aligned} \ddot{\boldsymbol{x}}(t) + \left(\tilde{\boldsymbol{B}} + \omega\tilde{\boldsymbol{G}}\right)\dot{\boldsymbol{x}}(t) + \\ + \left(\boldsymbol{\Lambda} + \omega^2\left(\tilde{\boldsymbol{K}}_\omega - \tilde{\boldsymbol{K}}_d\right) + \boldsymbol{V}^T\left(\sum_{s=1}^{p}\sum_{j=1}^{b}\boldsymbol{K}_{s,j}^C\right)\boldsymbol{V}\right)\boldsymbol{x}(t) &= \boldsymbol{V}^T\left(\omega^2\boldsymbol{f}_0 + \boldsymbol{f}(t)\right) . \end{aligned} \tag{23}$$

Matrices

$$\tilde{\boldsymbol{X}} = diag\left({}^m\boldsymbol{V}_D^T \boldsymbol{X}_D \, {}^m\boldsymbol{V}_D \, , \quad {}^m\boldsymbol{V}_R^T \boldsymbol{X}_R \, {}^m\boldsymbol{V}_R\right) \in \mathcal{R}^{m,m} \tag{24}$$

for $\boldsymbol{X} = \boldsymbol{G}, \boldsymbol{B}, \boldsymbol{K}_d, \boldsymbol{K}_\omega$ (with $\boldsymbol{K}_{\omega D} = \boldsymbol{0}$) and

$$\boldsymbol{\Lambda} = diag\left({}^m\boldsymbol{\Lambda}_D \, , \quad {}^m\boldsymbol{\Lambda}_R\right) \qquad \boldsymbol{V} = diag\left({}^m\boldsymbol{V}_D \, , \, {}^m\boldsymbol{V}_R\right) \tag{25}$$

is composed from spectral submatrices ${}^m\boldsymbol{\Lambda}_D \in \mathcal{R}^{m_D,m_D}$, ${}^m\boldsymbol{\Lambda}_R \in \mathcal{R}^{m_R,m_R}$ of the subsystems satisfying the conditions

$${}^m\boldsymbol{V}_D^T \boldsymbol{K}_{\mathbf{s}D} \, {}^m\boldsymbol{V}_D = {}^m\boldsymbol{\Lambda}_D \, , \quad {}^m\boldsymbol{V}_R^T\left(\boldsymbol{K}_{\mathbf{s}R} + \boldsymbol{K}_{PP}^C\right)^m \boldsymbol{V}_R = {}^m\boldsymbol{\Lambda}_R \, . \tag{26}$$

The vector $\boldsymbol{f}_0 = \left[\boldsymbol{f}_D^T \, , \, \boldsymbol{f}_C^T\right]^T$ expresses the influence of the centrifugal forces. The global vector of the aerodynamic forces is $\boldsymbol{f}(t) = \boldsymbol{f}e^{i\omega_k t}$, where $\boldsymbol{f} = \left[\boldsymbol{0}^T \; \boldsymbol{f}_R^T\right]^T$. We assume the harmonic blade excitation in axial (outspread to turbomachine rotor) and circumferential (tangential) direction concentrated in blade nodals i (Fig. 1) in the complex form

$$\boldsymbol{f}_{B,j}(t) = \left[\ldots ; F_{iy}\cos\varphi_{j,s} + iF_{iy}\sin\varphi_{j,s} ; F_{iz}\cos\psi_{j,s} + iF_{iz}\sin\psi_{j,s} ; \ldots\right] e^{i\omega_k t} , \tag{27}$$

where ω_k is dominant excitation frequency corresponding to number of stator nozzles multiply angular velocity of the rotating disk. The angle $\varphi_{j,s}$ is the phase angle of the aerodynamic forces acting on j-th blade in s-th blade packet in the axial direction and $\psi_{j,s}$ is the phase angle in tangential direction on the same blade. These phase angles can be expressed in the form

$$\varphi_{j,s} = \left[j - 1 + (s-1)3\right] 2\pi\frac{p_{SB}}{p_{MB}} \qquad \psi_{j,s} = \varphi_{j,s} - \varphi \, , \tag{28}$$

where φ is the relative phase shift between aerodynamic forces applied in axial and circumferential direction (see a contribution Misek et al., 2007) and p_{SB} (p_{MB}) is stator (rotor) blade number.

3. Forced vibration

We consider only aerodynamic forces acting on the moving blades, that's why we don't use below the constant centrifugal force $\boldsymbol{f}_0$ presented in (23). The steady dynamic response of the rotating bladed disk calculated at the condensed model (23) is of the form $\boldsymbol{x}(t) = \boldsymbol{x}e^{i\omega_k t}$ with complex amplitude vector

$$\boldsymbol{x} = \boldsymbol{Z}^{-1}\boldsymbol{V}^T\boldsymbol{f} \tag{29}$$

where

$$\boldsymbol{Z} = -\omega_k^2\boldsymbol{E} + i\omega_k\left(\tilde{\boldsymbol{B}} + \omega\tilde{\boldsymbol{G}}\right) + \left(\boldsymbol{\Lambda} + \omega^2\left(\tilde{\boldsymbol{K}}_\omega - \tilde{\boldsymbol{K}}_d\right) + \boldsymbol{V}^T\left(\sum_{s=1}^{p}\sum_{j=1}^{b}\boldsymbol{K}_{s,j}^C\right)\boldsymbol{V}\right) \tag{30}$$

is the dynamic stiffness matrix of the condensed model and $\boldsymbol{f}$ is vector of the complex amplitudes of the aerodynamic excitation. Damping matrix $\boldsymbol{B}$ is proportional to matrices of mass and static stiffness of subsystems D (disk) and R (rim). By using modal transformation we obtain the steady state solution in global configuration space

$$\boldsymbol{q}e^{i\omega_k t} = \boldsymbol{V}\boldsymbol{x}e^{i\omega_k t}. \tag{31}$$

This solution is in complex form and the real displacements of the exciting rotating bladed disk is the real part of the complex generalized coordinate vector

$$\boldsymbol{q}(t) = Re\{\boldsymbol{q}e^{i\omega_k t}\}. \tag{32}$$

4. Application

On the basis of the presented method the original software in MATLAB code was created. The matrices of the disk were obtained by three-dimensional finite element method as is shown in Šašek et al. 2006. The matrices of the blade rim were derived by one-dimensional finite element method applied to blades with shroud (Zeman & Kellner, 2006). The aerodynamic forces applied in axial and tangential direction on each moving blade were assumed from Misek et al. (2007). The software and the proposed approach was applied to the centrally clamped steel bladed disk of following basic parameters:

disk inner/outer radius	$0,335/05754\ m$
disk thickness	$0,155\ m$
length of blades	$0,253\ m$
width/thickness of shroud with rectangular profil	$0,1005/0,014\ m$
number of blades in packets b	3
number of blade packets p	18
DOF number of the discretized disk n_D	3240
DOF number of the discretized blade ring n_R	3672
Young's modulus of the disk, blade and shroud materials E	$2.10^{11}\ Pa$
Poisson's ratio ν	$0,3$
mass density ϱ	$7800\ kg.m^{-3}$

translation stiffnesses of the flexible blade seating in disk (Fig.1)

$$k_{x_j} = k_{z_j} = 2,8.10^9;\; k_{y_j} = 4,88.10^9 \; Nm^{-1}$$

torsional/flexural stiffnesses of the flexible blade seating in disk (Fig.1)

$$k_{x_jx_j} = 1,05.10^8;\; k_{y_jy_j} = 1,5.10^7 \;\; k_{z_jz_j} = 3.10^7 \; Nm.rad^{-1}$$

stiffnesses linkages between blade packets (Fig.1)

$$k_u = k_v = k_w = 10^9 \; Nm^{-1};\; k_\varphi = k_\psi = 10^7;\; k_\vartheta = 10^6 \; Nm.rad^{-1}$$

amplitude of global axial force F_y acting on one blade	$700\ N$
amplitude of global tangential force F_z acting on one blade	$1600\ N$
relative phase shift between F_y and F_z	25

The results of excited vibrations of rotating bladed disk are shown in Fig.3, Fig.4, Fig.5 and Fig.6. In Fig.3 there can be seen higher vibration round $1000\ rpm$ and in the end of investigated range $3000\ rpm$. This can be compared with axial blade node displacements in Fig.5, where the characteristic of blade packet vibration is shown. Important result is that the shroud moves less than the disk. It can be caused high exciting frequency ($3000\ rpm \;\rightarrow\; f_k = 2\pi\omega_k = 1600\ Hz$) of aerodynamic forces, which excites more disk due to two dog bolts between blades and disk.

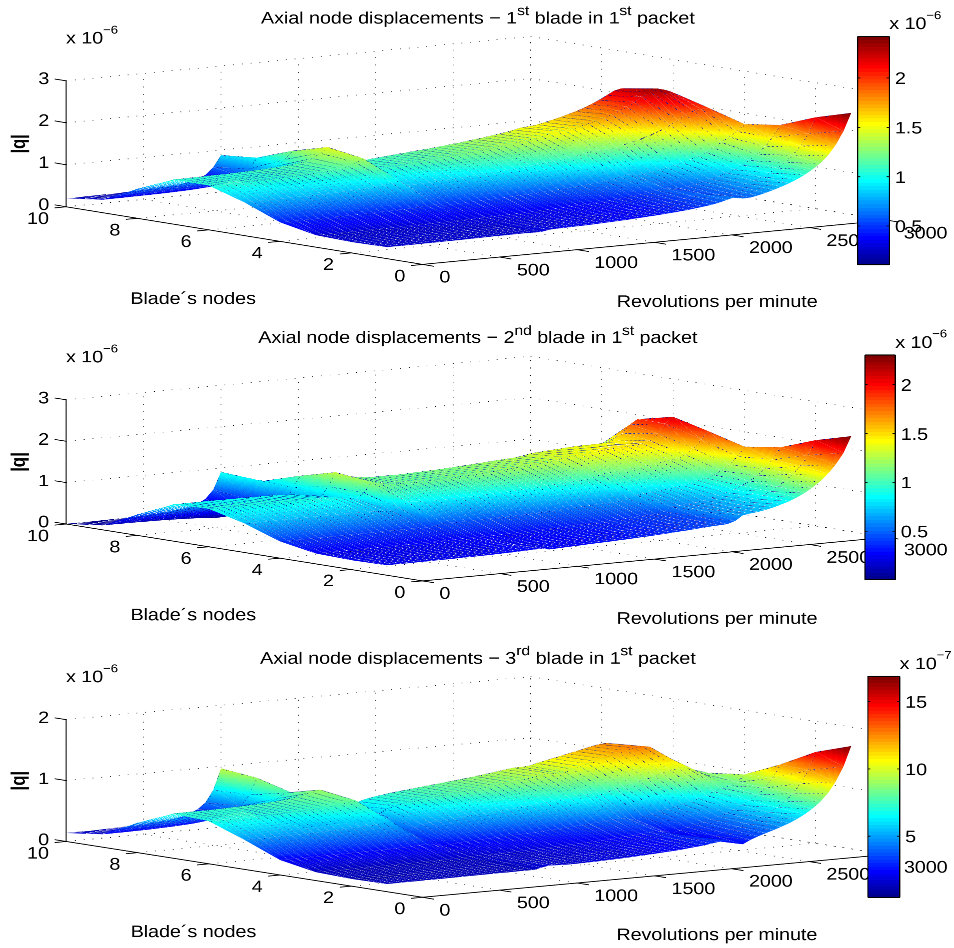

Figure 3: Amplitude characteristics of axial blade node displacements in the first packet.

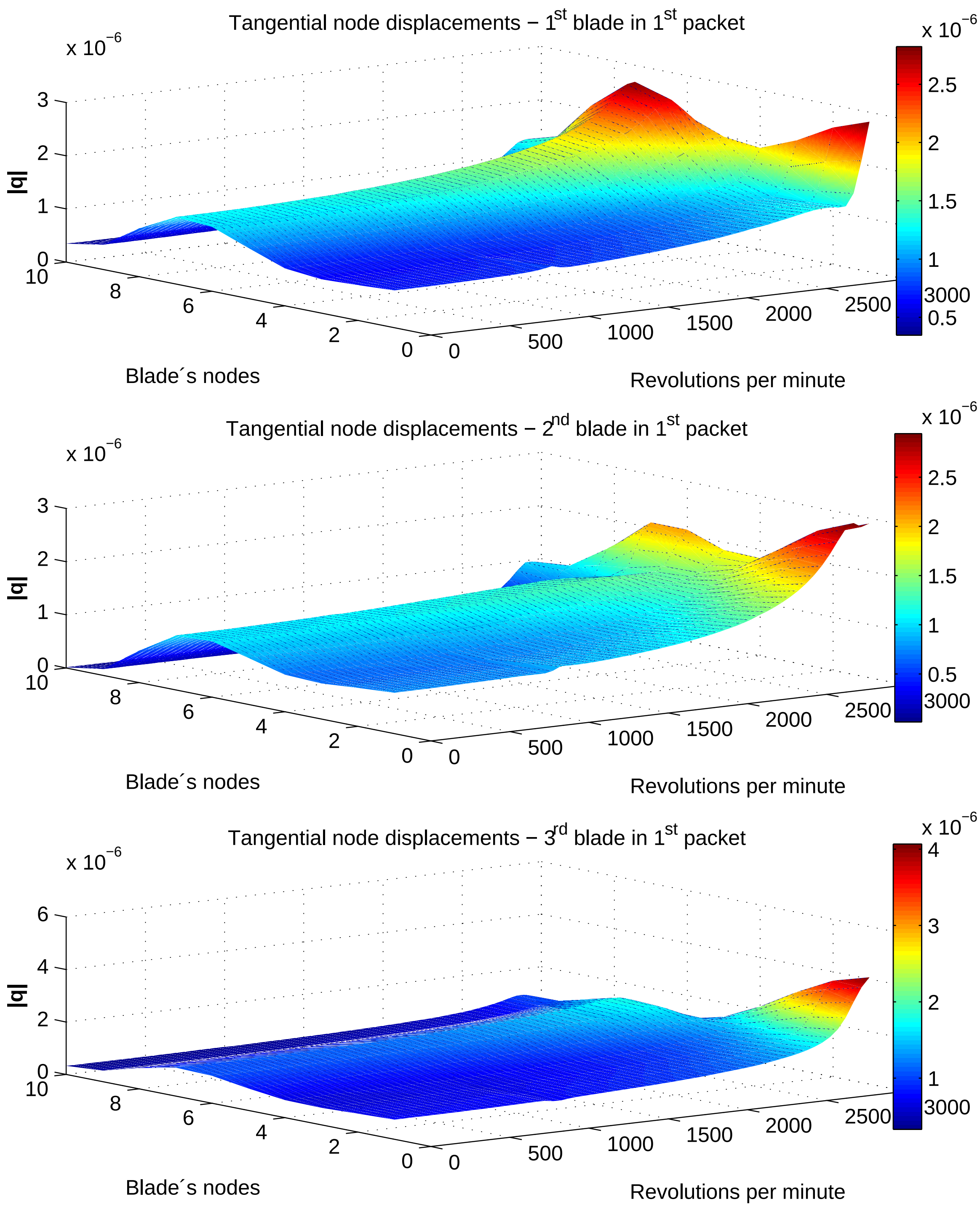

Figure 4: Amplitude characteristics of tangential blade node displacements in the first packet.

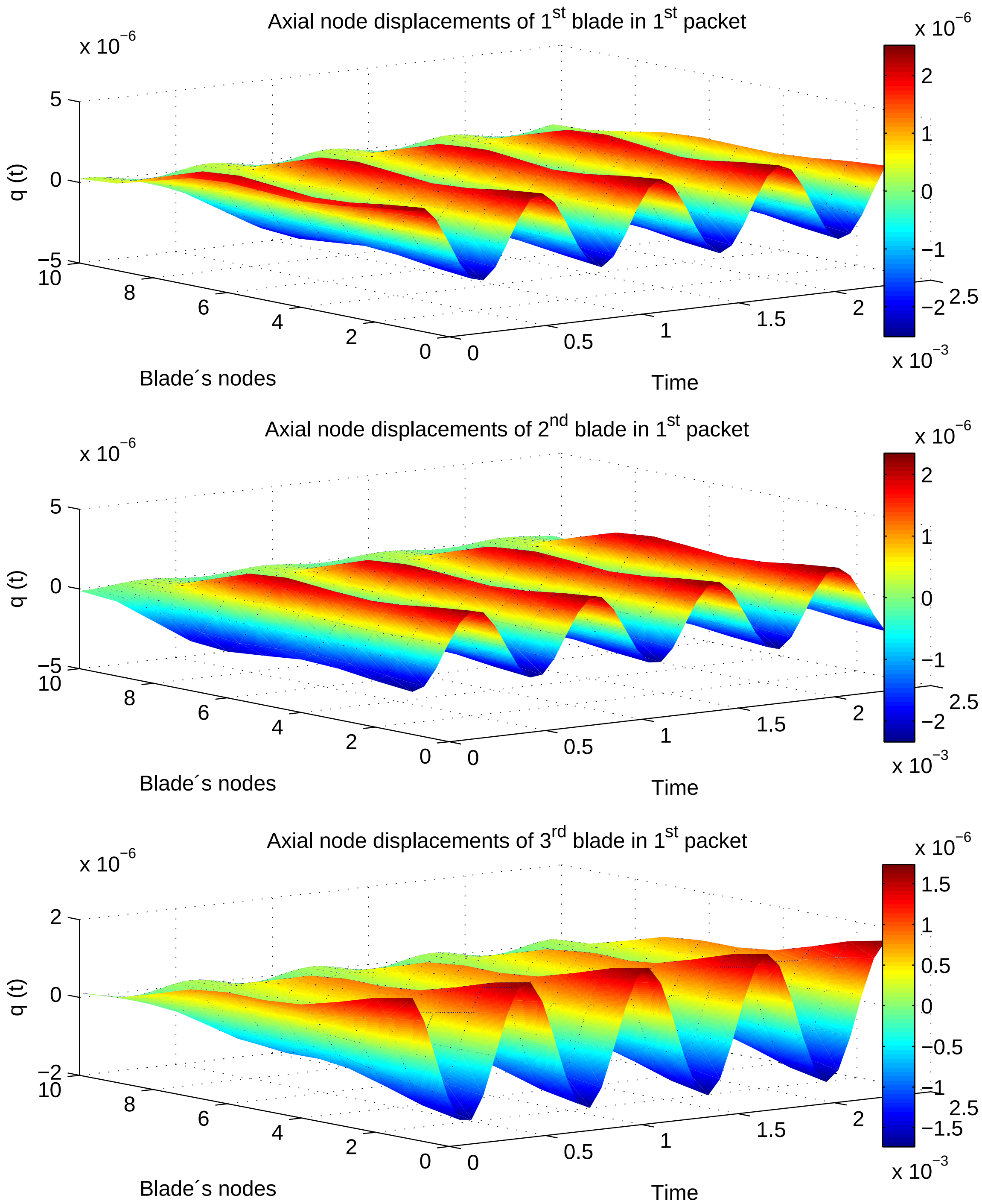

Figure 5: Time depend of axial blade node displacements in the first packet for $3000\ rpm$.

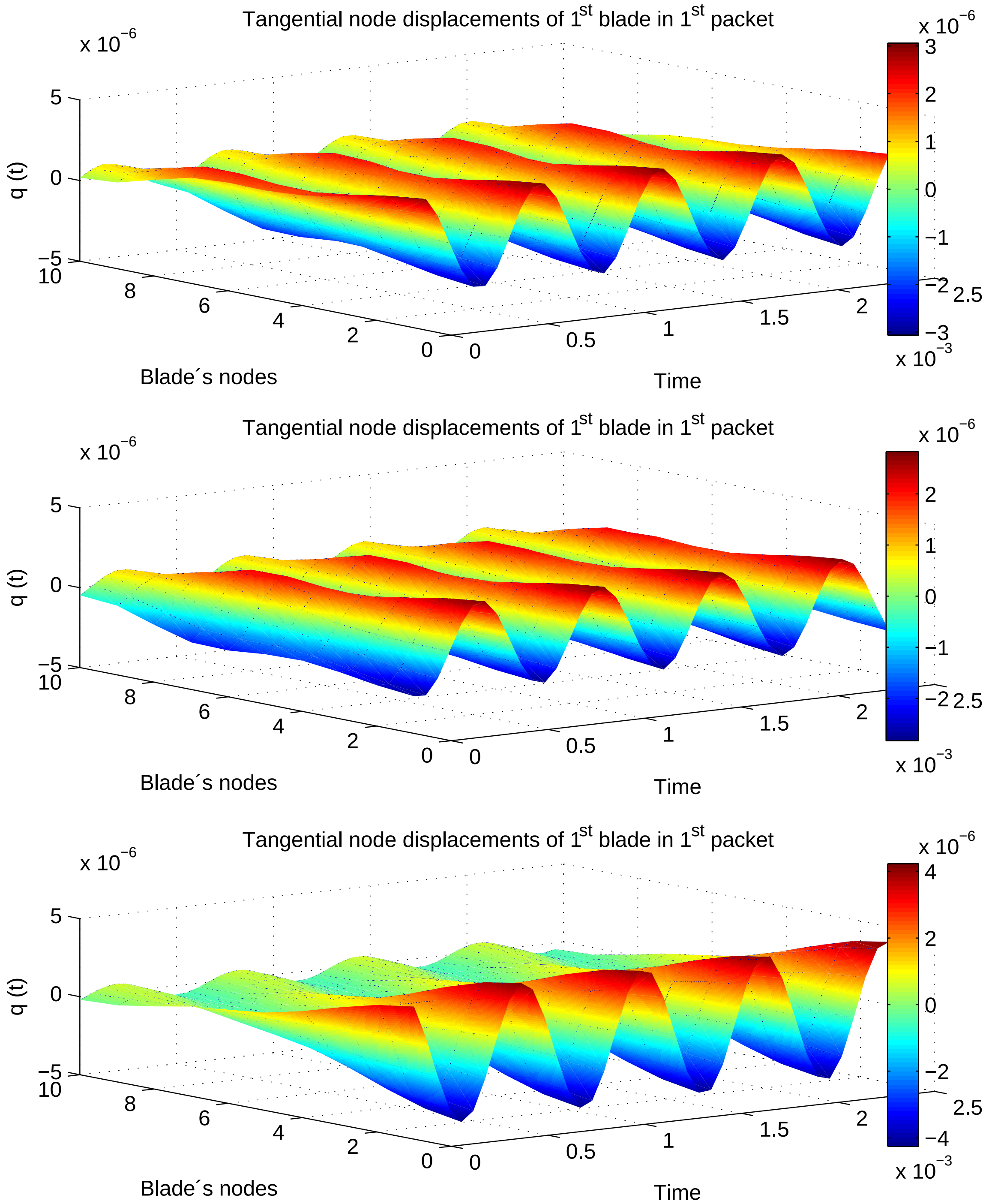

Figure 6: Time depend of tangential blade node displacements in the first packet for $3000\ rpm$.

5. Conclusion

The new methodology of the rotating bladed disk vibration is based on the system decomposition into subsystems – disk and blade rim – joined by discrete couplings. The mathematic model includes an influence of Coriolis and centrifugal forces on both subsystems, blade's elastic seating to rotating flexible disk, centrifugal blade stiffening, elastic linkages between a shroud of the blade packets and proportional damping of subsystems. The excitation forces acting along the moving blade length induced by steam flow (obtained from CFD analysis) are included. By using modal synthesis method the coupled system of disk and blade rim is condensed to calculate steady aerodynamic vibrations of the bladed disk. The method can be used in turbomachine dynamics.

6. Acknowledgement

This work was supported by the research project MSM 4977751303 and the Fund for University Development FRVS 23/2007.

7. References

Birget, R. (2001) Blades and Bladed Disks. *Encyklopedia of Vibration*, Academic Press, San Diego, Vol. 1. p. 174-179.

Genta, G. (2005) *Dynamics of Rotating Systems*. Springer Science & Bussines Media, Inc., New York.

Kellner, J. & Zeman, V. (2006) Influence of Dynamic Stiffness, Centrifugal Forces and Blade's Elastic Seating on Blade Modal Properties, in: *Proc. Applied Mechanics 2006*, University of West Bohemia in Pilsen, p. 47-48 (full text on CD-ROM).

Krämer, E. (1993) *Dynamics of Rotors and Foundations*. Springer-Verlag, Berlin.

Misek, T., Tetiva, A., Prchlik, L. & Duchek, K.(2007) Prediction of high cycle fatigue life of steam turbine blading based on unsteady CFD and FEM forced response calculation, in: *Proc. of ASME Turbo Expo 2007*, Montreal (accepted for publication).

Šašek, J., Zeman, V. & Hajžman, M. (2006) Modal Properties of Rotating Disks, in: *Proc. Computational Mechanics 2006*,(J. Vimmr editor), University of West Bohemia in Pilsen, Vol. 2, p. 593-600.

Yamamoto, T. & Ishida, Y. (2001) *Linear and Nonlinear Rotordynamics, A Modern Treatment with Applications*. John Wiley & Sons, New York.

Zeman, V. (2005) Usage of Modal Synthesis in Modelling Tuning and Optimization of Large Vibrating Mechanical Systems, in: *Proc. Computing of Strucuture by Finite Element Method*, (V. Laš editor), University of West Bohemia in Pilsen, p. 133-142 (in Czech).

Zeman, V. & Kellner, J. (2006) Mathematical Modelling of Bladed Disk Vibration, in: *Proc. Computational Mechanics 2006*, (J. Vimmr editor), University of West Bohemia in Pilsen, Vol. 2, p. 713-720 (in Czech).

Zeman, V., Kellner, J. & Šašek, J. (2007) Contribution to modelling of bladed disk vibration, in: *Proc. Dynamics of Machines 2007* (L. Pešek editor), Institute of Termomechanics AS ČR, pp. 213-220.